Старший научный сотрудник ТОО «PlasmaScience»; e-mail: satbaeva.z@mail.ru. ORCID: https://orcid.org/0000-0001-7161-2686.

Айбек Бакытжанович Шынарбек – докторант специальности «Механика и метталообработка»; НАО «Университета имени Шакарима города Семей», Республика Казахстан; ведущий научный сотрудник ИЦ «Упрочняющие технологии и покрытия»; e-mail: shinarbekov16@mail.ru. ORCID: https://orcid.org/0009-0009-2877-5178.

Дастан Маратұлы Жасболатов – магистрант факультета «Высшая школа науки и технологий» Ниигатский университет, Япония; e-mail: dastanzhas01@gmail.com.

Received 18.02.2025
Revised 05.03.2025
Accepted 06.03.2025

https://doi.org/10.53360/2788-7995-2025-1(17)-44

IRSTI: 29.19.15

B.K. Rakhadilov[1], R.K. Kussainov[2], R.K. Kurmangaliyev [2], M.N. Azlan[3], N.E. Musataeva[2]*
[1]LLP «Plasma Science»,
070018, Republic of Kazakhstan, Ust-Kamenogorsk, Gogol str. 7G
[2]Engineering Center «Strengthening Technologies and Coatings»,
071412, Republic of Kazakhstan, Semey, Fizkulturnaya str., 4a,
[3]Universiti Pendidikan Sultan Idris,
Tanjong Malim, 35900, Perak, Malaysia
*e-mail: naziramusataeva51@gmail.com

THEORETICAL STUDIES OF THERMAL PROCESSES IN ELECTROLYTIC-PLASMA HARDENING

Abstract: *This article examines the theoretical aspects of thermal processes occurring during electrolytic-plasma hardening (EPH), including the analysis of temperature fields and heating rates. The finite difference method was used for numerical modeling, allowing for a more precise determination of the temperature distribution in the treated material. The heat transfer problem in a flat plate with a thickness of 15 mm was considered, where the boundary conditions were as follows: on one boundary, heating was carried out by a surface thermal flux from the electrolyte plasma, while on the opposite side, heat was dissipated through convection in an air medium. The calculations revealed non-uniform temperature distribution over time and depth, confirming the formation of three distinct structural zones: the hardened zone, the heat-affected zone, and the base matrix. The temperature of the samples during the experiment was measured using a thermocouple positioned 2 mm from the heated surface. Experimental data obtained from the treatment of 45 steel samples confirmed the accuracy of the numerical modeling. The research results demonstrate the effectiveness of numerical modeling, including the finite difference method, in optimizing EPH parameters, thereby reducing the volume of experimental work and lowering technology development costs. The obtained data can be used to improve surface hardening technologies for structural steel components used in agricultural machinery, mechanical engineering, and other industries. The study confirms the potential of EPH for enhancing the operational characteristics of steel products.*

Key words: *Electrolytic-plasma hardening, 45 steel, heat conduction equation, numerical modeling, thermal processes.*

Introduction

Modern material processing technologies are aimed at improving their operational properties, such as hardness, wear resistance, corrosion resistance, and high-temperature stability. One of the promising heat treatment methods that allow achieving these goals is electrolytic-plasma hardening (EPH). This method combines the effects of plasma discharge and electrolysis, enabling not only structural modifications of the material's surface layer but also diffusion saturation with various elements such as carbon, nitrogen, and boron.

EPH is widely applied in mechanical engineering, aviation, and the automotive industry, where increased strength and durability of components operating under high mechanical and thermal loads are required. However, the effectiveness of this method largely depends on the correct selection of

processing parameters, such as electrolyte composition, voltage, electrode dimensions, and cooling rate.

This study focuses on the influence of electrolytic-plasma hardening parameters on the properties of 45-grade structural steel, which is extensively used in the manufacturing of agricultural machinery components. Special attention is given to the theoretical study of electrolyte conductivity and thermal processes occurring during EPH, as well as the numerical modeling of temperature fields in treated materials.

The objective of this work is to determine the optimal conditions for electrolytic-plasma processing that ensure maximum surface hardening of steels while minimizing deformations and preserving the geometric parameters of components. To achieve this, theoretical calculations, numerical modeling, and experimental studies were conducted, and their results are presented in this article.

The relevance of this study is driven by the need to enhance the efficiency and precision of heat treatment processes, which is particularly important in the manufacturing of working components subjected to increased loads. The research findings can be used to optimize technological processes in mechanical engineering and other industrial sectors.

An essential aspect of developing heat treatment technologies is considering the thermophysical properties of materials, such as thermal conductivity, heat capacity, and thermal diffusivity. These properties determine how a material responds to thermal exposure and influence the final characteristics of the treated surface. In particular, thermal conductivity coefficients play a key role in heating and cooling processes, which is especially important when processing materials that operate under high-temperature conditions.

A study on the thermal conductivity coefficients of stainless steel 12X18H10T over a wide temperature range has shown that the material's thermal conductivity significantly changes with increasing temperature, which must be taken into account when designing technological processes [1]. These findings align with the results presented in the work "Thermophysical Properties of Metals at High Temperatures", which describes in detail the dependence of various metals' thermophysical properties on temperature [2]. Accounting for these dependencies enables more accurate modeling of heating and cooling processes, which is particularly crucial for electrolytic-plasma processing, where surface temperatures can reach 1400°C or higher.

Another important factor affecting the service life of components is the wear intensity of structural materials. As shown in the study by M.Yu. Kolobov, S.V. Vorobyov, E.V. Mironov, E.Yu. Kuvaeva, S.E. Sakharov, V.V. Kolobova on the impact of technological parameters of equipment on the wear intensity of structural materials (to be included in the references), properly selected processing parameters-such as heating rate, processing time, and electrolyte composition-can significantly reduce wear and increase the durability of components [3]. This study also examines the relationship between EPH process parameters and the wear intensity of steel 45, providing recommendations for optimizing processing conditions to enhance wear resistance.

To refine the technological parameters of electrolytic-plasma processing, this study conducted numerical modeling of temperature fields in 45-grade steel. Currently, this method allows obtaining computational results that align well with analytical solutions and experimental data. During electrolytic-plasma hardening, concentrated energy fluxes induce intense heating of the component, leading to a rapid temperature increase. According to various estimates, the heat flux density can reach 3×10^3 W/cm², which is sufficient to heat a steel sample to 1400 °C. This often results in surface melting, and excessive heating durations may cause deformation of the treated component. Therefore, numerical modeling is advisable to refine the technological parameters of electrolytic-plasma hardening before processing and to reduce the volume of experimental studies.

The use of modern computational methods, such as the finite difference method, provides high accuracy in predicting temperature distribution within the material depth while considering the influence of different processing parameters. The results of numerical modeling are also compared with experimental data to verify the model's accuracy, making this approach a reliable tool for calculating thermal processes in various applications.

Thus, the results of this study contribute to the development of material hardening technologies and can be used to improve the operational characteristics of components in various industries. Considering the thermophysical properties of materials, such as thermal conductivity and diffusivity, along with the influence of process parameters on wear intensity, allows for the optimization of

electrolytic-plasma processing and enhances the durability of components operating under high-stress conditions. The research findings are consistent with data from studies on the thermophysical properties of metals and the impact of processing parameters on material wear, confirming the relevance and practical significance of the conducted research.

Research Methods

Numerical modeling of local heating for 45-grade steel components was conducted for the case of electrolytic-plasma processing (EPP) using a 50kW installation [4], and the obtained calculation results were compared with experimental temperature data measured using a thermocouple. For the study, steel 45 plates (70×50×15 mm³) were selected as the material (Figure 1). The chemical composition of 45-grade steel is presented in Table 1.

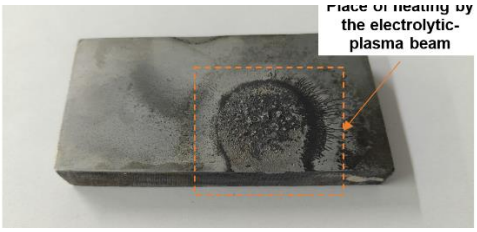

Figure 1 – Steel plate heated by EPH

Before processing, the surface of the samples was leveled using a TROJAN GP-1A grinding machine, followed by manual finishing on a flat glass surface using abrasive sandpaper. The grinding process was performed in stages, starting with coarse sandpaper (grit P100) and finishing with finer sandpaper (grit P2500). Residual grinding marks were eliminated by polishing on an unstretched fabric using a paste containing dispersed chromium oxide particles.

Table 1 – Chemical Composition of 45 Steel

C (Carbon)	Si (Silicon)	Mn (Manganese)	P (Phosphorus)	S (Sulfur)	Cr (Chromium)	Ni (Nickel)	Cu (Copper)	Fe (Iron)
0,42-0,5	0,17-0,37	0,5-0,8	< 0,03	< 0,035	< 0,25	< 0,30	< 0,30	other

This study investigates the heat transfer problem in a metal plate of finite thickness L. For a semi-infinite body, calculations were performed using an analytical formula. In the case of a plate with finite thickness L, assuming that the heating (or cooling) process occurs in one direction, the mathematical model is described by the one-dimensional heat conduction equation:

$$\rho c_p \frac{\partial T}{\partial t} = \lambda \frac{\partial^2 T}{\partial x^2} \quad (1)$$

where ρ is the density of the material, c_p - is the specific heat capacity, λ - is the thermal conductivity coefficient, and T(x,t) - represents the temperature at point x at time t. The plate occupies the interval $[0, L]$ along the x-axis. It is assumed that the initial condition is given as

$$T(x, t) = T_0,$$

indicating that at the initial moment, the temperature of the plate is equal to the ambient temperature T_0.

Solving the heat conduction problem allows determining the temperature distribution $T(x, t)$ across the thickness of the plate over time. Based on this, other physical quantities such as the heating rate $\frac{\partial T}{\partial t}$, can be calculated, or the temperature at a specific point x can be determined.

Numerical calculations were performed using the Python programming language in the PyCharm 2024.3 environment, utilizing libraries for mathematical computations and data visualization. The work was conducted on a 64-bit Windows 11 operating system.

The heat conduction calculation algorithm for a plate of finite thickness L consists of several steps. First, the user specifies the thermophysical properties of the material (ρ, cp, λ), the plate thickness L, the step sizes for coordinate Δx and time Δt, as well as initial and boundary conditions (e.g., heat flux q_0, its duration τ, convection coefficient h, ambient temperature $Tenv$, and other parameters).

$$Fo = \alpha \frac{\Delta t}{(\Delta x)^2} < 0.5 \quad (2),$$

where $\alpha = \lambda / \rho\, c_p$.

Next, arrays are created to store the coordinates x (from 0 to L with step Δx) nd the initial temperature distribution $T(x,0)$. A time loop is then executed (from $t=0$ to $t=max$ with step Δt). At each time step, for all internal nodes $i=1,\dots,N_{x-2}$ the explicit finite difference scheme is applied:

$$T_i^{n+1} = T_i^n + Fo(T_{i+1}^n - 2T_i^n + T_{i-1}^n) \quad (3).$$

The scheme of the solved problem is shown in figure 2.

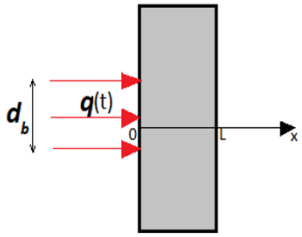

Figure 2 – Heat conduction problem scheme for a flat plate made of steel 45

During the calculations, the program generates an array T_i^n, which stores temperature values depending on the coordinate and time. The results are visualized using the Matplotlib library:

1) A temperature map $T(x,t)$ in a color scale,
2) Graphs of temperature distribution $T(x)$ at different moments in time.
3) Temperature variation curves $T(t)$ at fixed points.

Thus, the mathematical model represents a classical boundary-value problem for the heat conduction equation. The Python-based program is implemented using an explicit finite-difference scheme, which takes into account realistic or assigned boundary conditions for heating and cooling. The obtained results allow comparing calculated data with analytical solutions and experimental measurements. If necessary, the grid parameters (Δx, Δt) can be adjusted or boundary conditions can be modified over time, for instance, by terminating the heat flux at a specific moment τ.

Numerical modeling is based on solving the heat conduction equation using the finite-difference method with an explicit scheme. This approach allows for a detailed calculation of the temperature field in a metallic plate of finite thickness. It is assumed that the plate interacts with the surrounding air, which imposes additional boundary conditions: On one surface, a heat flux $q(t)$ (e.g., from an electrolytic plasma heat source) is applied. On the opposite surface, convective heat exchange with air occurs. This methodology provides a comprehensive description of thermal processes in the material, considering not only internal heat conduction but also heat dissipation into the surrounding medium. By selecting appropriate spatial Δx and temporal Δt step sizes that satisfy stability criteria, it becomes possible to dynamically track how heat propagates from the heated surface to deeper layers and subsequently dissipates when the heat source is turned off. The outcome of the modeling is the temperature field $T(x,t)$ and its evolution over time.

The general form of the heat conduction equation is written as:

$$\rho c_p \frac{\partial T}{\partial t} = \lambda \frac{\partial^2 T}{\partial x^2} + Q(x,t), \quad (4)$$

where: ρ – density of the material, c_p – specific heat capacity, λ – thermal conductivity coefficient, T – temperature, $Q(x,t)$ – volumetric heat source (electrolytic plasma beam) (W/m³).

The equation is solved using the explicit finite-difference scheme:

$$\rho c_p \frac{T_i^{n+1} - T_i^n}{\Delta t} = \lambda \frac{T_{i+1}^n - 2T_i^n + T_{i-1}^n}{(\Delta x)^2}.$$

The boundary conditions for the heat conduction problem are defined as follows:

– At the left boundary *x=0* a heat flux *q(t)* (W/m²) is applied:

$$-\lambda \frac{\partial T}{\partial x}|_{x=0} = q(t). \quad (5)$$

– At the right boundary $x=L$, where the plate is in contact with still air at room temperature $Tenv = 20$, the Newton's Law of Cooling describes the convective heat transfer:

$$-\lambda \frac{\partial T}{\partial x}|_{x=L} = h\,(T(L,t) - T_{env}). \quad (6)$$

Where h — is the heat transfer coefficient, which for natural convection in still air is typically 10 W/(m²·K).

The initial condition is given as:

$$T(x,0) = T_0, \tag{7}$$

where T_0 — is the initial temperature of the sample.

The discretization steps for the coordinate Δx and time Δt in the explicit finite difference scheme must satisfy the stability criterion, which is expressed through the Fourier number as $Fo < 0.5$:

$$Fo = \frac{\lambda \Delta t}{\rho\, c_p\, (\Delta x)^2} < 0.5. \tag{8}$$

where:

$$\alpha = \frac{\lambda}{\rho\, c_p}.$$

This criterion ensures that for a fixed spatial step Δx a sufficiently small time step Δt, must be chosen to prevent numerical instability. If the condition $Fo < 0.5$ is not met, approximation errors may accumulate rapidly, leading to incorrect simulation results. Therefore, adhering to this stability criterion is crucial for ensuring the accuracy of the temperature distribution calculations over time and space.

Results and Discussion

Figures 3 and 4 present graphs of temperature variations in the sample over time and across its thickness, calculated using the finite difference method.

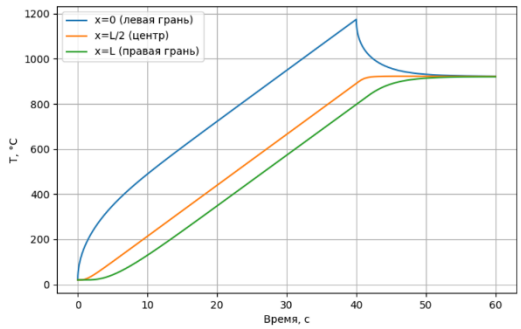

Figure 3 – Graph of temperature change in the sample

In Figure 4, the x-axis represents time $t(\mathrm{c})$, while the y-axis represents temperature $T(°C)$. The graph contains three curves corresponding to different points within the plate: $x = 0$ – the left surface in contact with the electrolytic-plasma beam source; $x = L/2$ – the midpoint of the sample, $x = L$ – the right surface, where heat dissipates into the air due to convection.

The graph shows that the temperature at the left boundary reaches its maximum value towards the end of the heating phase at $t = 40$ c after which it begins to decrease. In contrast, the center of the sample and the right boundary experience a gradual increase in temperature, which continues even after heating has stopped, as heat propagates deeper into the material. By $t = 60$ c the temperature becomes uniform across all points.

Figure 3 depicts the temperature distribution T as a function of depth z (mm) for different time intervals. Each curve corresponds to a specific time moment. It is evident that over time, the surface at $x = 0$, for different time intervals. Each curve corresponds to a specific time moment. It is evident that over time, the surface at $x = 15$ mm, the temperature is lower and barely increases at the initial moments. However, as time progresses, the temperature profile gradually rises, indicating heat diffusion into the material. After the electrolytic-plasma beam heating stops (at $t = 45$ s and $t = 55$ s) the temperature equalizes across the sample. Interestingly, beyond $x = 6{,}5$ mm the temperature exceeds that at $t = 40$ s, which is explained by continued heat transfer from the left to the right boundary after heating has stopped.

For comparison, Figure 5 presents the temperature distribution across the depth of the sample during cooling, obtained using an analytical method based on the equation [8]:

$$T(z,t) = \frac{2 \cdot A \cdot q_0}{\lambda} \cdot \left[\sqrt{a \cdot t} \cdot ierfc\left(\frac{z}{2 \cdot \sqrt{a \cdot t}}\right) - \sqrt{a(t-\tau)} \cdot ierfc\left(\frac{z}{2\sqrt{a \cdot (t-\tau)}}\right)\right], \tag{9}$$

where: t – current time $(t > \tau)$,τ – heating duration.

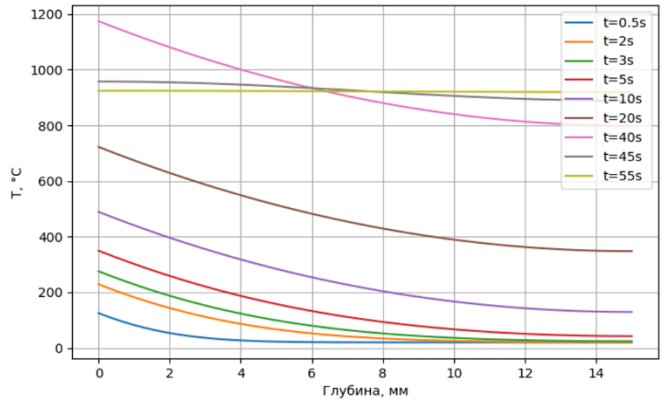

Figure 4 – Graph of temperature distribution along the depth of the part

This formula describes the temperature distribution $T(z,t)$ through the functions $\sqrt{a \cdot t}$ and $ierfc\left(\frac{z}{2 \cdot \sqrt{a \cdot t}}\right)$). It assumes a semi-infinite medium model and does not account for heat reflection from the opposite boundary or complex boundary conditions. At large time values and greater depths, the temperature stabilizes into a plateau when the formula limits heating to $t > \tau$. This leads to smooth but eventually converging curves after heating ceases.

The main difference between the two approaches is that the analytical method is applicable for a semi-infinite body or cases with a limited heating time condition $t > \tau$. In contrast, the finite difference method accounts for the finite thickness of the sample and the boundary conditions at the opposite surface, allowing a more realistic description of temperature behavior at longer times and deeper regions of the material.

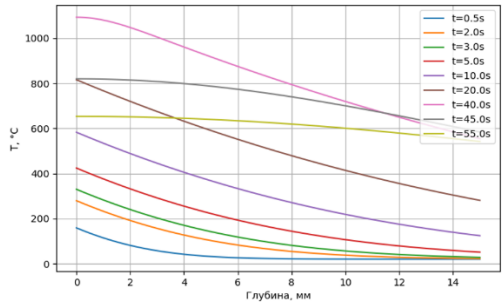

Figure 5 – Graphs of temperature distribution along the depth at different moments during and after heating

Figure 6 presents the heating rate field, calculated using the finite difference method. The graph illustrates how the heating rate $\frac{\partial T}{\partial t}$ evolves considering the finite thickness of the plate and realistic boundary conditions. In the initial phase (up to 5 s), the maximum heating rate is observed near the heated surface, due to intensive thermal exposure. As heat propagates deeper, the active heating zone shifts, and at longer times, the heating rate decreases as heat dissipates within the material.

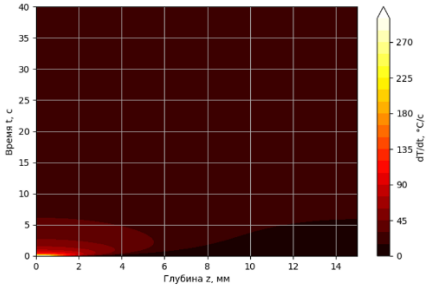

Figure 6 – Temperature distribution field along the depth of the part, calculated using the finite difference method

The results presented in Figure 6 indicate that the finite difference method provides a more precise reflection of the influence of the second boundary of the plate, especially at longer time values t. The analytical approach for a semi-infinite body produces a smooth heating rate distribution, but it does not account for heat exchange effects at the opposite boundary, leading to a more extended and less pronounced heating zone in the region $z > 10$ мм. Similar conclusions can be drawn from the analysis of the heating rate graph across the depth of the sample, presented in Figure 7.

In Figure 7, it is evident that at the moment heating is turned off, the heating rate at the surface sharply transitions into the negative region, indicating the cooling process. This is due to the consideration of the finite thickness of the sample and realistic boundary conditions at the opposite boundary.

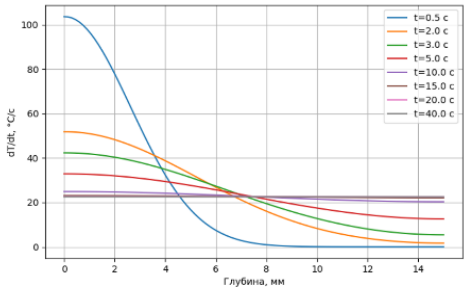

Heating rate along the depth of the part, calculated using the finite difference method

Figure 7 – Graph of heating rates along the depth of the part

Table 2 presents the experimental data of the average temperature measured in four steel 45 plate samples at a distance of 2 mm from the heated surface. The data include both theoretical and experimental temperature values at different time intervals.

Table 2. – Experimental Temperature Data of Steel 45 Plate at 2 mm Distance from the Heated Surface

№	Time, s	Temperature, °C	
		Theoretical Calculation	Experiment
1	0	20	20
2	0,5	91,22	50
3	2	146,64	180
4	3	190,85	200
5	5	262,44	250
6	10	400,32	420
7	15	519,79	620
8	20	635,25	700
9	30	864,06	900
10	40	1092,34	1050
11	45	963,94	940
12	50	940,03	800
13	55	934,46	780
14	60	932,85	700

Theoretical results (represented by black squares in Figure 8) closely align with experimental data (red circles) during the initial heating phase (up to $t = 10$ s). However, between 10-20 s, there is a noticeable deviation: the numerical method underestimates the temperature values compared to the experimental results. At $t = 40$ s, the model predicts a higher peak temperature (1090°C), whereas the experiment recorded a maximum temperature of 1050°C. During the cooling phase (40-60 s), the calculated temperature decreases more slowly than the experimental data: in experiments, the temperature drops to 700-800°C, while in theoretical calculations, it remains at 930-940°C.

Possible reasons for these discrepancies include simplifications in the mathematical model (e.g., not accounting for heat loss due to radiation or incomplete consideration of convective heat transfer) and experimental measurement errors (e.g., abrupt switching off of the heat source or sensor placement issues). However, the overall heating and cooling dynamics remain sufficiently accurate, confirming the model's applicability for engineering assessments.

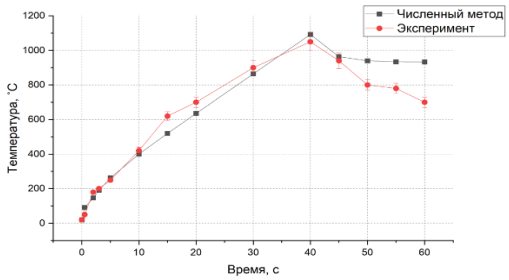

Figure 8 – Graph of heating rates along the depth of the part

Additionally, the temperature distribution within the sample promotes the formation of three main structural zones during heat treatment: quenching zone, thermal influence zone, base matrix.

Conclusion

In this article, a theoretical study of thermal processes during EPH of structural steel 45 has been conducted. The main focus was on the analysis of temperature fields and heating rates, as well as numerical modeling of temperature distribution in the processed material.

For solving the heat transfer problem, numerical calculations using the finite difference method were applied. The results of numerical modeling showed that the heating rate could reach 200°C/s, which contributes to the formation of a martensitic structure with enhanced hardness. Non-uniform temperature distribution over time and depth was identified, confirming the existence of three structural zones: the quenching zone, the thermal influence zone, and the base matrix. The analytical method, while applicable for a semi-infinite body, does not account for the finite thickness of the sample and complex boundary conditions, making it less accurate in describing real-world processes.

Experimental data, obtained from processed steel 45 samples, confirmed the accuracy of numerical modeling, although some discrepancies were noted due to simplifications in the model and measurement errors. The finite difference method, considering finite plate thickness and boundary conditions on the opposite side, provided a more realistic description of temperature behavior at longer times and deeper material layers.

The study demonstrated the effectiveness of numerical modeling for optimizing EPH parameters, which allows for reducing the volume of experimental work and lowering costs in technology development. The obtained data can be used to improve surface hardening technologies for structural steel parts used in agricultural machinery, mechanical engineering, and other industries.

Thus, the study confirms the promising application of electrolytic-plasma hardening for improving the performance characteristics of steel products, such as hardness, wear resistance, and high-temperature durability. Taking into account thermophysical properties of materials and processing parameters enables optimization of EPH processes and enhancement of component durability operating under high loads.

References

1. Thermal conductivity coefficients of stainless steel 12X18H10T in a wide temperature range / S.V. Stankus et al // High-Temperature Thermophysics. – 2008. – Vol. 46, № 5. – P. 795-797.
2. Zinoviev V.E. Thermophysical properties of metals at high temperatures / V.E. Zinoviev // Handbook. – Metallurgy, 1989.
3. Influence of equipment process parameters on the wear intensity of structural materials / M.Yu. Kolobov et al // Russian Chemical Journal. – 2023. – Vol. 67, № 1. – P. 64-69.
4. Influence of plasma-electrolytic hardening regimes on the structure and properties of 65G steel / B.K. Rakhadilov et al // Eurasian Journal of Physics and Functional Materials. – 2021. – Vol. 5, № 3. – P. 209-221.
5. Belkin P.N. Plasma-electrolytic hardening of steels: Review / P.N. Belkin, S.A. Kusmanov // Surface Engineering and Applied Electrochemistry. – 2016. – Vol. 52, № 6. – P. 531-546.
6. Influence of electrolytic-plasma surface hardening on the structure and strength properties of ferrite-pearlite class steel for wheels / B.K. Rakhadilov et al // Eurasian Journal of Physics and Functional Materials. – 2020. – Vol. 4, № 2. – P. 167-173.
7. Kusainov R.K. et al. Application of electrolytic-plasma hardening to improve the properties of machine parts made of steel 45.

8. Chepachenko Yu.I. Finite difference method for solving the heat conduction equation. – 2012.
9. Konyaeva N.I. Review of methods for restoring worn-out tillage machine parts / N.I. Konyaeva, N.V. Konyaev // Modern Materials, Equipment, and Technologies. – 2023. – № 1 (46). – P. 60-a.
10. Influence of electrolytic-plasma surface hardening on the structure and properties of 40XH steel / G.M. Toktarbaeva et al // Bulletin of the East Kazakhstan State Technical University named after D. Serikbayev. – 2020. – № 1. – P. 199-204.
11. Rakhadilov B.K. Improving the wear resistance of automatic coupler device parts through electrolytic-plasma surface hardening / B.K. Rakhadilov, Ye. Kyzyrkhan, L.G. Zhurerova // Bulletin of the East Kazakhstan State Technical University named after D. Serikbayev. – 2016. – № 3. – P. 117-121.
12. Bobanova Zh.I. Wear-resistant galvanic coatings based on iron alloys / Zh.I. Bobanova, S.P. Sidelnikova, D.M. Kroitoru // Electronic Processing of Materials. – 2004. – № 1. – P. 18-24.
13. Gadiyeva S.S. Application of finite difference methods for solving model heat and mass transfer equations / S.S. Gadiyeva, P.F. Gakhramanov // Bulletin of the Dagestan State University. Series 1: Natural Sciences. – 2017. – Vol. 32, № 4. – P. 38-46.
14. Kobychev A.A. Study of the heat conduction equation using the finite difference method / A.A. Kobychev, V.A. Kobychev, N.N. Karavaeva. – 2010.
15. Popov N.M. Investigation of an algorithm for solving the heat conduction differential equation using the finite difference method / N.M. Popov // Automation and Energy Saving in Mechanical Engineering, Energy, and Transport. – 2022. – P. 236-241.
16. Modification of the surface of 30KhGSA steel using electrolytic-plasma thermocyclic hardening / B.K. Rakhadilov et al // New Materials and Technologies: Powder Metallurgy, Composite Materials, Protective Coatings, Welding. – 2022. – P. 610-616.

Б.К. Рахадилов[1], Р.К. Кусаинов[2], Р.Х. Курмангалиев[2], М.Н. Азлан[3], Н.Е. Мусатаева[2*]
[1]ТОО «Plasma Science»,
070000, Республика Казахстан, г. Усть-Каменогорск, ул. Гоголя, 7Г
[2]Инжиниринговый центр «Упрочняющие технологий и покрытия»,
Университет имени Шакарима города Семей,
071412, Республика Казахстан, г. Семей, ул. Физкультурная, 4а,
[3]Universiti Pendidikan Sultan Idris, Tanjong Malim,
35900, Перак, Малайзия
*e-mail: naziramusataeva51@gmail.com

ТЕОРЕТИЧЕСКИЕ ИССЛЕДОВАНИЯ ТЕПЛОВЫХ ПРОЦЕССОВ ПРИ ЭЛЕКТРОЛИТНО-ПЛАЗМЕННОЙ ЗАКАЛКЕ

В статье рассмотрены теоретические аспекты тепловых процессов, происходящих при ЭПУ, включая анализ температурных полей и скоростей нагрева. Для численного моделирования использован метод конечных разностей, что позволило более точно определить распределение температуры в обрабатываемом материале. Рассматривалась задача теплопереноса в плоской пластине толщиной 15 мм, при котором граничные условия были следующими: на одной границе производился нагревание поверхностным тепловым потоком электролитной плазмы, с противоположной стороны тепло отводилось за счет конвекции в воздушной среде. Расчеты показали неравномерность распределения температуры по времени и глубине, что подтверждает возникновения трех разных структурных зон: зоны закалки, зоны термического воздействия и основной матрицы. Температура образцов при эксперименте измерялась с помощью термопары на расстоянии 2 мм от нагреваемой поверхности. Экспериментальные данные, полученные при обработке образцов из стали марки 45, подтвердили корректность численного моделирования. Результаты исследования демонстрируют эффективность использования численного моделирования, включая метод конечных разностей, для оптимизации параметров ЭПУ, что сокращает объем экспериментальных работ и снижает затраты на разработку технологий. Полученные данные могут быть использованы для совершенствования технологий упрочнения поверхностей деталей из конструкционных сталей, применяемых в сельскохозяйственной технике, машиностроении и других отраслях промышленности. Исследование подтверждает перспективность применения ЭПУ для повышения эксплуатационных характеристик стальных изделий.

Ключевые слова: *Электролитно-плазменное упрочнение, сталь 45, уравнение теплопроводности, численное моделирование, тепловые процессы.*

Б.К. Рахадилов[1], Р.К. Кусаинов[2], Р.Х. Курмангалиев[2], М.Н. Азлан[3], Н.Е. Мусатаева[*2]
[1]«Plasma Science" ЖШС,
070000, Қазақстан Республикасы, Өскемен қаласы, Гоголь көшесі, 7Г
[2]«Беріктендіру технологиялары мен жабындары» инженерлік орталығы,
Шәкәрім атындағы Семей университеті,
071412, Қазақстан Республикасы, Семей қ., дене шынықтыру к-сі, 4а
[3]Universiti Pendidikan Sultan Idris, Tanjong Malim,
35900, Перак, Малайзия
[*]e-mail: naziramusataeva51@gmail.com

ЭЛЕКТРОЛИТТІК-ПЛАЗМАЛЫҚ СӨНДІРУДЕГІ ЖЫЛУ ПРОЦЕСТЕРІН ТЕОРИЯЛЫҚ ЗЕРТТЕУ

Бұл мақалада ЭПУ кезінде жүретін жылу процестерінің теориялық аспектілері, оның ішінде температуралық өрістер мен қыздыру жылдамдықтарын талдау қарастырылған. Сандық модельдеу үшін соңғы айырмалар әдісі қолданылып, материалдағы температураның таралуын дәлірек анықтауға мүмкіндік берді. Жылу тасымалдау мәселесі қалыңдығы 15 мм болатын жазық пластина үшін қарастырылды, онда шекаралық шарттар келесідей болды: бір жағында электролиттік плазманың беткі жылу ағынымен қыздыру жүргізілді, ал қарама-қарсы жағында жылу ауа ортасы арқылы конвекция есебінен әкетілді. Есептеулер температураның уақыт пен тереңдік бойынша біркелкі бөлінбейтінін көрсетті, бұл үш түрлі құрылымдық аймақтың пайда болуын дәлелдейді: шынықтыру аймағы, термиялық әсер ету аймағы және негізгі матрица. Эксперимент кезінде үлгілердің температурасы қыздырылатын беттен 2 мм қашықтықта термопара көмегімен өлшенді. 45 маркалы болат үлгілерін өңдеу нәтижесінде алынған эксперименттік деректер сандық модельдеудің дұрыстығын растады. Зерттеу нәтижелері электролиттік-плазмалық шынықтыру параметрлерін оңтайландыру үшін соңғы айырмалар әдісін қоса алғанда, сандық модельдеуді қолданудың тиімділігін көрсетті, бұл эксперименттік жұмыстардың көлемін қысқартып, технологияларды әзірлеу шығындарын азайтуға мүмкіндік береді. Алынған деректер ауыл шаруашылығы техникасында, машина жасауда және өнеркәсіптің басқа салаларында қолданылатын құрылымдық болаттан жасалған бөлшектердің беттерін нығайту технологияларын жетілдіру үшін пайдаланылуы мүмкін. Зерттеу ЭПУ-ды болат бұйымдардың жұмыс сипаттамаларын, соның ішінде қаттылықты, тозуға төзімділікті және жоғары температураларға төзімділікті арттыру үшін қолданудың перспективалы әдіс екенін растайды.

Түйін сөздер: *Электролиттік-плазмалық шынықтыру, 45 маркалы болат, жылу өткізгіштік теңдеуі, сандық модельдеу, жылу процестері.*

Information about the authors

Bauyrzhan Rakhadilov – PhD, Vice-rector on scientific work of Sarsen Amanzholov East Kazakhstan University, Ust-Kamenogorsk, Kazakhstan; e-mail: rakhadilovb@mail.ru.

Rinat Kenzheevich Kusainov – Head of the Engineering Center «Strengthening Technologies and Coatings», Semey, Kazakhstan; e-mail: rinat.k.kus@mail.ru.

Rinat Khamituly Kurmangaliev – Junior Researcher at the Engineering Center «Strengthening Technologies and Coatings», Semey, Kazakhstan; e-mail: rinat_real@rambler.ru.

Muhammad Noorazlan Bin Abd Azis – PhD, Associate Professor, Nano Center, Faculty of Science and Mathematics, Universiti Pendidikan Sultan Idris, Tanjong Malim, Perak, Malaysia; e-mail: azlanmn@fsmt.upsi.edu.my.

Nazira Musataeva* – Student of the F-302 group, Shakarim University of Semey, Kazakhstan; e-mail: naziramusataeva51@gmail.com.

Авторлар туралы ақпарат

Бауыржан Рахадилов – PhD, Сәрсен Аманжолов атындағы Шығыс Қазақстан университетінің ғылыми жұмыс жөніндегі проректоры, Өскемен, Қазақстан; e-mail: rakhadilovb@mail.ru.

Ринат Кенжеұлы Құсаинов – «Берік технологиялар және жабындар» инженерлік орталығының жетекшісі, Семей, Қазақстан; e-mail: rinat.k.kus@mail.ru.

Ринат Хамитұлы Құрманғалиев – «Берік технологиялар және жабындар» инженерлік орталығының кіші ғылыми қызметкері, Семей, Қазақстан; e-mail: rinat_real@rambler.ru.

Мұхаммад Нуразлан Бин Абд Азис – PhD, доцент, Наноорталық, Ғылым және математика факультеті, Сұлтан Идрис атындағы Білім беру университеті, Танжонг Малим, 35900, Перак, Малайзия; e-mail: azlanmn@fsmt.upsi.edu.my.

Назира Мусатаева* – F-302 тобының студенті, Шәкәрім атындағы Семей университеті, Қазақстан; e-mail: naziramusataeva51@gmail.com.

Информация об авторах

Бауржан Рахадилов – PhD, проректор по научной работе Восточно-Казахстанского университета имени Сарсена Аманжолова, Усть-Каменогорск, Казахстан; e-mail: rakhadilovb@mail.ru.

Ринат Кенжеевич Кусаинов – руководитель Инжинирингового центра «Упрочняющие технологии и покрытия», Семей, Казахстан; e-mail: rinat.k.kus@mail.ru.

Ринат Хамитулы Курмангалиев – младший научный сотрудник Инжинирингового центра «Упрочняющие технологии и покрытия», Семей, Казахстан; e-mail: rinat_real@rambler.ru.

Мухаммад Нуразлан Бин Абд Азис – PhD, доцент, Наноцентр, факультет науки и математики, Университет образования султана Идриса, Танджонг Малим, Перак, Малайзия; e-mail: azlanmn@fsmt.upsi.edu.my.

Назира Мусатаева* – студентка группы F-302, Университет имени Шакарима города Семей, Казахстан; e-mail: naziramusataeva51@gmail.com.

Received 26.02.2025
Revised 03.03.2025
Accepted 04.03.2025

https://doi.org/10.53360/2788-7995-2025-1(17)-45

МРНТИ: 61.51.00

Е.Н. Мясоедова*, Ж.К. Алдажуманов, Д.В. Мясоедов, А.Н. Шалаганова, А.Е. Сатыбалдинова
Университет имени Шакарима города Семей,
071410, Республика Казахстан, г. Семей, ул. Глинки 20А
*e-mail: Kate_white89@mail.ru

СРАВНИТЕЛЬНЫЙ АНАЛИЗ РАДИАЦИОННОГО ИЗЛУЧЕНИЯ РАЗЛИЧНЫХ МОДЕЛЕЙ ТЕЛЕФОНОВ

Аннотация: *Статья посвящена сравнительному анализу радиационного излучения, которое исходит от различных моделей мобильных телефонов. Целью исследования является определение уровней излучения, а также их соответствие допустимым нормам, установленным международными стандартами. В рамках работы были проведены дозиметрические измерения, позволяющие оценить интенсивность излучения каждой модели, а также выявить возможные отклонения от предельно допустимых значений. Сравнение телефонов проводилось по ключевым показателям, таким как величина специфической поглощённой мощности (SAR) и уровень ионизирующего излучения. Уделено особое внимание методологии измерений, чтобы обеспечить точность и воспроизводимость результатов. Дополнительно в статье рассматриваются факторы, влияющие на уровень излучения, такие как конструктивные особенности телефонов, частотные диапазоны и условия эксплуатации. Приведённый анализ позволяет выявить закономерности между техническими характеристиками устройств и их радиационной безопасностью. Полученные данные могут быть полезны не только для конечных пользователей, а также и для производителей, стремящихся к созданию более безопасных устройств. Работа подчеркивает важность информирования населения о потенциальных рисках, связанных с излучением мобильных телефонов, и предлагает практические рекомендации для их минимизации.*

Ключевые слова: *излучение телефонов, ионизирующее излучение, негативное воздействие, дозиметрия, допустимые нормы.*

Введение

Мобильный телефон представляет собой портативное устройство, основная функция которого заключается в обеспечении голосовой связи. Сегодня сотовая связь является наиболее популярным видом мобильной радиосвязи, поэтому термин "мобильный телефон" зачастую ассоциируется именно с сотовым устройством. Это изобретение можно поставить в один ряд с важнейшими достижениями человечества, такими как печатный станок и автомобиль. Если книгопечатание дало возможность сохранять и распространять знания, а автомобиль значительно расширил границы передвижения, то мобильный телефон позволил людям оставаться на связи практически в любой точке планеты и в любое время [1].